

# Far infrared and Ultraviolet emissions of individual galaxies at $z=0$ : selection effects on the estimate of the dust extinction

V. Buat<sup>1,2</sup>, J. Donas<sup>1</sup>, B. Milliard<sup>1</sup>, C. Xu<sup>3</sup>

<sup>1</sup> IGRAP, Laboratoire d'Astronomie Spatiale du CNRS, BP 8, 13376 Marseille Cedex 12, France

<sup>2</sup> Laboratoire des interactions photons-matière, Faculté des Sciences de Saint Jérôme, 13397 Marseille Cedex 13, France

<sup>3</sup> California Institute of Technology, Pasadena, CA 91125, USA

Received; accepted ....

**Abstract.** We have cross-correlated Far Infrared (IRAS) and UV (FOCA) observations of galaxies to construct a sample of FIR selected galaxies with a UV observation at  $0.2 \mu\text{m}$ .

The FIR and UV properties of this sample are compared to the mean properties of the local Universe deduced from the luminosity distributions at both wavelengths. Almost all the galaxies of our sample have a FIR to UV flux ratio larger than the ratio of the FIR and UV luminosity densities, this effect becoming worse as the galaxies become brighter: the increase of the UV ( $0.2 \mu\text{m}$ ) extinction is about 0.5 mag per decade of FIR ( $60 \mu\text{m}$ ) luminosity.

Quantitative star formation rates are estimated by adding the contribution of the FIR and UV emissions. They are found consistent with the corrections for extinction deduced from the FIR to UV flux ratio. A total local volume-average star formation rate is calculated by summing the contribution of the FIR and UV wavelengths bands. Each band contributes for an almost similar amount to the total star formation rate with  $\rho_{\text{SFR}} = 0.03 \pm 0.01 \text{ h} \cdot \text{M} \odot / \text{yr} / \text{Mpc}^3$  at  $z=0$ . This is equivalent to a global extinction of 0.75 mag to apply to the local luminosity density at  $0.2 \mu\text{m}$ .

The trend of a larger FIR to UV flux ratio for a larger FIR luminosity found for our sample of nearby galaxies is extended and amplified toward the very large FIR luminosities when we consider the galaxies detected by ISOCAM in a CFRS field and the Ultra Luminous Infrared Galaxies at low and high redshift. A UV extinction is tentatively estimated for these objects.

**Key words:** Infrared: galaxies–Ultraviolet: galaxies–Galaxies: luminosity function–Galaxies: statistics

## 1. Introduction

The problem of internal dust extinction in galaxies is difficult whereas its estimate is crucial for understanding the evolution of the Star Formation Rate from high redshift to now. At high  $z$  the emission observed in the visible corresponds to the UV rest frame where the effects of the dust extinction can be dramatic. For example the shape of the Madau plot (e.g. Madau et al. 1998) depends a lot on the extinction adopted as a function of the redshift. Since the work of Calzetti, Kinney and collaborators from IUE data (e.g. Kinney et al. 1993, Calzetti et al. 1994) the slope of the UV continuum in the range  $1200\text{--}2600 \text{ \AA}$  ( $f_{\lambda} \propto \lambda^{\beta}$ ) has been identified as a powerful indicator of the dust extinction. The reason is that only short lived stars contribute substantially to the emission in this wavelength range and the intrinsic shape of the spectrum is only sensitive to the recent star formation history. For example  $\beta$  reaches a steady value  $\sim -2$  as soon as the star formation rate has been constant for some  $10^7$  years (Calzetti et al. 1994). An instantaneous starburst represents the most extreme case of a steep spectrum with  $\beta$  equal to  $-2.7$  (Meurer et al. 1995). Once an intrinsic value for  $\beta$  is adopted any deviation from this value is interpreted in terms of dust extinction which flattens the intrinsic slope. At high redshift  $\beta$  is observable in the visible wavelength range and this has conferred a large interest to this approach.

Nevertheless, at least two difficulties arise when using this method: on the one hand the choice of an intrinsic UV slope  $\beta$  (i.e. of a star formation history) can modify substantially the amount of extinction and has led to some discrepancies in the estimate of the extinction which can reach 1-2 mag in UV (Pettini et al. 1998, Meurer et al. 1997, Steidel et al. 1999, Calzetti 1997); on the other hand if the deviation of  $\beta$  from its intrinsic value is indubitably a dust extinction tracer, deriving a quantitative value of the extinction from this deviation is difficult due to the various unknown factors like geometry or dust properties intervening in the estimate of the extinction (e.g. Calzetti et al. 1994). The quantification of the extinction is easier

on nearby galaxies which can be obviously used as templates. The empirical approach of Calzetti and collaborators (Calzetti et al. 1994, Kinney et al. 1994, Calzetti 1997) had the advantage of providing a global attenuation curve for starburst galaxies accounting for geometrical effects in a statistical way.

Another powerful approach lies in making global energetic considerations. Indeed, for nearby templates, it is possible to perform a total energetic budget since the dust emission of these galaxies is almost always known from IRAS observations. Such considerations have led to quantitative estimates of the extinction (Buat & Xu 1996, Meurer et al. 1999). Recently, Meurer et al. (1999) have related the FIR to UV flux ratio and the UV slope  $\beta$  to the extinction at 1600 Å. Their unreddened UV spectrum has a slope of -2.23 intermediate between a constant star formation rate and an instantaneous burst.

Uncertainties about the UV extinction are already present at low redshifts. Meurer et al. (1999) find an extinction around 1.8 mag at 1600 Å for the starburst templates observed by IUE whereas we find 1.3 mag at 2000 Å for a sample of nearby starburst galaxies (Buat & Burgarella 1998) and around 0.8 mag for more quiescent disk galaxies (Buat & Xu 1996). The difference is likely to be due at least in part to the properties of the individual galaxies used for these studies but also to different assumptions about the dust absorption as it will be discussed below.

We need to know how to correct individual galaxies for extinction but also how the properties of these individual cases can be extrapolated to the entire population of galaxies. This problem is especially important at high  $z$  since as we go farther only the brightest objects become visible. With the availability of the luminosity functions at various wavelengths we have now the possibility to test if the results deduced from the properties of individual galaxies are representative of the mean characteristics deduced from the local luminosity functions.

The basic idea of this paper is to compare the FIR (60 and 100  $\mu\text{m}$ ) and UV(0.2 $\mu\text{m}$ ) of a sample of nearby galaxies for which selection biases are well known. The sample will be FIR selected and the aim is to study how much these individual galaxies thus selected trace the mean properties of the local universe. After a presentation of our IRAS/FOCA sample (section 2), we discuss the FIR and UV properties of the individual galaxies in terms of extinction and selection biases in section 3. The section 4 is a comparison with the luminosity functions at both wavelengths. In section 5 we derive quantitative star formation rates from the FIR and UV emissions. Endly, in section 6 we compare the FIR and UV properties of Ultra Luminous Infrared Galaxies both at low and high redshift and of the ISOCAM detections of intermediate redshift galaxies in a CFRS field with those of our IRAS/FOCA

sample of nearby galaxies.

## 2. The IRAS/FOCA sample

### 2.1. Construction of the sample of galaxies

The FOCA balloon borne wide-field UV camera (Milliard et al. 1994) has observed a cumulated sky surface of  $\sim 100$  square degrees in a 150Å wide band-pass centered near 0.2  $\mu\text{m}$ . The camera (a 40-cm Cassegrain telescope with an image intensifier coupled to a IlaO emulsion film) was operated in two modes, the FOCA 1000 (f/2.6) and FOCA 1500 (f/3.8), which provide 2.3 deg field of view, 20'' resolution, and 1.5 deg field of view, 12'' resolution, respectively. The typical limiting depth in one hour observing time is  $m(0.2\mu\text{m}) = 18.5$  where the magnitude is defined by  $m(0.2\mu\text{m}) = -2.5 \log f - 21.175$  where the flux  $f$  is in  $\text{erg}/\text{cm}^2/\text{s}/\text{Å}$  (Donas et al. 1991). Here we have considered the 22 calibrated fields ( $\sim 70$  square degrees), in order to cross correlate them with the observations of the IRAS satellite. Table 1 gives the coordinates of the guide star (near the field center), the total exposure time and the size for each field.

The infrared objects of the IRAS Faint Sources Catalog (FSC) have been associated to sources from other astronomical catalogs. Such cross-correlations are very useful to determine the nature of the sources detected. Unfortunately only a small proportion of UV sources have an identification in an other catalog. So we have chosen to start from the IR detections for which much data are available and to search for their UV counterparts. *Therefore our sample will be FIR selected.*

For each UV field, we have extracted the FIR sources detected by IRAS at 60 and/or 100 microns and listed in the IRAS FSC. This has been done using the VIZIER facility of the Centre de Données astronomiques de Strasbourg (CDS). 364 IR sources have been selected.

Since we are only interested by the extragalactic targets we have kept only the objects associated to known galaxies from the catalog of associations of the FSC. 102 from the 364 sources at 60 or 100 microns have been securely identified as galaxies. We have only kept galaxies which are not confused with a neighbored source present in cross-correlated catalogs

Then we have searched for a UV source matching each FIR detection of a galaxy in a circle of 45 arcsec radius centered on the IRAS coordinates. 94 galaxies have been identified both in UV and FIR. 8 FIR sources identified as galaxies have no UV counterpart. Few cases of several UV sources present in the circular area have been judged doubtful and discarded.

To avoid a contamination in the IR detection only galaxies with a cirrus flag lower than or equal to 2 are selected as adviced in the IRAS Faint Source Catalog. We are then left with 80 galaxies with a UV measurement and with 8

**Table 1.** Fields at  $0.2 \mu\text{m}$  observed by the FOCA experiment with the coordinates of the field center (guide star), the total exposure time in each field and the size of the field (diameter)

Field number	$\alpha$ (1950) h m s	$\delta$ (1950) d m s	Exposure FOCA1000	time (s) /FOCA1500	Field diameter deg
12	00 34 43.9	+40 03 27	1200	/	2.3
54	03 46 58.4	+22 05 37	600	/	2.3
10	08 17 26.1	+20 54 25	1400	/	2.3
51	08 48 36.0	+43 54 51	600	/800	2.3
18	08 51 57.6	+78 20 18	600	/	2.3
82	09 58 57.0	+69 01 41	2400	/	2.3
67	11 42 45.5	+20 10 03	600	/1600	2.3
33	11 59 04.1	+65 13 04	2000	/	2.3
81	12 19 29.2	+47 27 34	600	/	2.3
71	12 18 16.7	+15 49 06		/800	1.5
50	12 25 09.4	+08 53 13	450	/	2.3
34	12 26 02.3	+12 23 39	1800	/	2.3
28	12 57 08.1	+28 20 06	3000	/	2.3
30	13 03 47.1	+29 17 48	3000	/1200	2.3
31	13 09 32.4	+28 07 52	1050	/	2.3
96	13 29 50.2	+47 29 28		/1200	1.5
90	13 39 52.9	+28 37 38	300	/3600	2.3
29	14 01 04.2	+54 54 21		/1200	1.5
91	15 16 01.9	+02 15 51		/1200	1.5
89	15 36 52.8	+34 50 13		/3600	1.5
36	16 39 16.7	+36 17 46		/800	1.5
39	17 15 35.0	+43 11 21		/1200	1.5

galaxies detected by IRAS and not identified in UV. Endly we exclude nearby ellipticals and S0 galaxies present in our sample since we are only concerned by star forming galaxies. Very extended galaxies like M101 or M51 are excluded from the study since the photometry of these objects needs a special treatment. Our final sample contains 76 galaxies.

Complementary data necessary to the study of this sample like the optical identification, the B magnitude, the distance modulus are taken from the LEDA and NED databases. The fluxes are corrected for Galactic extinction using the Milky Way extinction curve of Pei (1992). Throughout the paper  $h$  will be defined as  $H_0/100 \text{ km s}^{-1}\text{Mpc}^{-1}$ .

## 2.2. The galaxies not detected at $0.2 \mu\text{m}$

8 galaxies detected by IRAS at least at  $60 \mu\text{m}$  do not appear in our UV frames. For one of them (F15451+0132), the non detection is explained by the fact that the galaxy is located on the edge of the UV image. Another source, F13038+2919, lies on the wings of the UV bright guide star (spectral type A3,  $m(0.2\mu\text{m}) < 7.3$ ). The UV identification of F12041+6519 (identified as MCG 11-15-022 in NED) at 60 arcsecs from the IRAS coordinates is quite uncertain. In table 2 are gathered the galaxies for which we can estimate an upper limit for their UV flux and F12041+6519 whose identification is uncertain. These

galaxies are faint even in FIR: 4 of them are only detected at  $60 \mu\text{m}$  with a very low flux.

*F13041+2907* and *F11431+2037* have no optical counterpart, *F13041+2907* is also detected at 1.4 GHz by FIRST (NED database).

*F12259+1141*, *F12235+0914* and *F12242+0919* are three galaxies located in the Virgo cluster area and identified by Yuan et al. (1996): *F12259+1141* (VCC1099) is a faint galaxy classified as dE; *F12242+0919* (VCC0934) a background blue galaxy classified Sa with a radial velocity equal to 6938 km/s; F12235+0914 is identified as VCC0864 and classified as Im or dE.

## 3. The FIR to UV flux ratio of individual galaxies

### 3.1. The FIR to UV flux ratio as an indicator of dust extinction

The FIR to UV ratio in star forming galaxies is now well recognized as a powerful indicator of extinction. The basic idea is to perform an energetic budget: the amount of stellar emission lost due to the extinction is re-emitted by the dust in the FIR. Nevertheless the quantitative calibration relies on models. In galaxies with an active star formation activity the heating of the dust is mostly due to the emission of young and massive stars; therefore the FIR to UV flux ratio is expected to be tightly related to the extinction. Following this approach, Buat and Xu (1996) have estimated the

**Table 2.** Galaxies detected in FIR with no or an uncertain UV detection. The B magnitude are taken from Yuan et al. 1996 and the CDS database.

IRAS name	$f(60\mu\text{m})$ Jky	$f(100\mu\text{m})$ Jky	$m_B$ mag	$m(0.2\mu\text{m})$ mag	$\log(F_{60}/F_{0.2})$	$a_{UV}$ mag
F11431+2037	0.329	< 0.72		> 18.5	> 1.82	> 3.8
F12041+6519	0.206	0.60	17	17.2	1.11:	2.3:
F12235+0914	0.260	< 0.94	15	> 17.2	> 1.21	> 2.6
F12242+0919	0.331	< 0.96	14.75	> 17.2	> 1.32	> 2.7
F12259+1141	0.266	< 1.92	18.4	> 18.5	> 1.72	> 3.8
F13041+2907	0.297	0.53		> 18.5	> 1.77	> 3.6

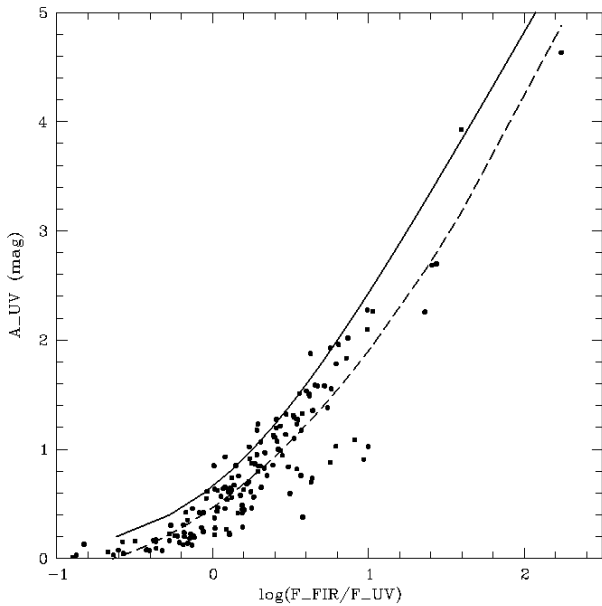


**Fig. 1.** The extinction in the UV wavelength range as a function of the ratio of the FIR and UV emissions. The points are the results of Buat and Xu (1996) and the UV fluxes are taken at  $0.2 \mu\text{m}$ , the dashed curve is the result of the polynomial fit to the points. The solid curve is obtained using the relation of Meurer et al. (1999) between the extinction and the FIR to UV ratio at  $0.16 \mu\text{m}$ .

extinction at  $0.2 \mu\text{m}$  in star forming galaxies using a radiation transfer model. Meurer et al. (1999) have followed a more empirical way to relate the FIR to UV ratio to the extinction at  $0.16 \mu\text{m}$  using a dust screen model and various extinction curves. They obtained a relation between the extinction and the FIR to UV flux ratio and then between the extinction and the UV slope  $\beta$ .

The results of both studies are compared in figure 1. The FIR flux is taken in the range  $40\text{-}120 \mu\text{m}$  as a combination of the emission at  $60$  and  $100 \mu\text{m}$  (Helou et al. 1988) and the UV flux is defined as  $F_\lambda = \lambda \cdot f_\lambda$  where  $f_\lambda$  is a flux per unit wavelength.

The extinction estimated by the model of Meurer et al. is calculated using their relation between the FIR to UV flux ratio and the extinction:

$$a_{0.16} = 2.5 \log\left(\frac{F_{\text{FIR}}}{1.19F_{0.16}} + 1\right)$$

It is shown as the solid curve in figure 1.

The results found by Buat and Xu (1996) for their sample of nearby galaxies are also reported in figure 1. A polynomial fit on the individual points gives:

$$a_{0.2} = 0.466(\pm 0.024) + 1.00(\pm 0.06) \log(F_{\text{FIR}}/F_{0.2}) \\ + 0.433(\pm 0.051) \log(F_{\text{FIR}}/F_{0.2})^2$$

The fit is reported as the dotted curve in figure 1.

We must account for the difference in wavelengths used in the two studies. First, we discuss the difference between the UV flux of galaxies at  $0.2$  or  $0.16 \mu\text{m}$  which affects the x-axis of the figure 1. Deharveng et al. (1994) have found the fluxes at  $0.165 \mu\text{m}$  of a sample of nearby galaxies systematically higher by 29% than the fluxes at  $0.2 \mu\text{m}$ . Adopting this result, the definition of the UV fluxes as  $F_\lambda = \lambda \cdot f_\lambda$  almost cancels the effect of wavelength and we can consider the fluxes at  $0.16$  and  $0.2 \mu\text{m}$  as similar.

The extinctions at  $0.16 \mu\text{m}$  and  $0.2 \mu\text{m}$  ( $a_{0.16}$  and  $a_{0.2}$ ) plotted along the y-axis of the figure 1 can also be considered as similar: their ratio is expected to vary from 0.9 to 1.1 using the extinction curve of the MW, LMC (Pei 1992) or that of Calzetti (1997). Therefore we will note both values as  $a_{UV}$  without any correction.

The UV extinctions derived from the two methods when the FIR to UV flux ratio of a galaxy is known are tightly correlated (correlation coefficient 0.99) since both are directly related to this FIR to UV flux ratio: the calculations of Meurer et al. lead to an extinction systematically larger than ours. The difference is  $\sim 0.2$  mag for low FIR to UV flux ratio ( $F_{\text{FIR}}/F_{UV} < 1.5$ ) and reaches  $\sim 0.4$  mag for  $F_{\text{FIR}}/F_{UV} > 5$ . This difference may arise from the different assumptions and calculations made in the two studies. Since they are interested by starburst galaxies Meurer et al. use a galaxy spectrum obtained from a constant star formation rate for at most  $10^8$  years whereas we use empirical broadband spectra: the contribution of the old evolved stars to dust heating is certainly larger

in our approach leading to a lower UV extinction for the same amount of dust emission. Another major difference is the treatment of geometrical effects. Meurer et al. use a screen model and we calculate the extinction with a radiation transfer model in an infinite plane parallel geometry where dust and stars are uniformly distributed and which accounts for scattering effects and disk inclination (Xu & Buat 1995). Finally we assume a Milky Way extinction curve whereas Meurer et al. adopt a uniform UV extinction for the entire spectrum of the starburst. Therefore, our model is probably more appropriate for normal star-forming galaxies and the entire disk of starburst galaxies whereas the calculations of Meurer et al. are made for starburst regions. Given these fundamental differences and the rather large uncertainties on the corrections for extinction the two methods are in reasonable agreement. The FIR to UV flux ratio appears relatively insensitive to the dust characteristics (type, distribution) and the stars/dust geometry. This has been confirmed by the recent study of Witt & Gordon (1999) who explore various dust distributions (homogeneous or clumpy), extinction properties (Milky Way or Small Magellanic Cloud) and stars/dust distributions (uniform mixture or shells). Such a robustness makes the FIR to UV flux ratio a reliable quantitative tracer of the dust attenuation in star forming galaxies.

### 3.2. The variation of the FIR to UV ratio: the influence of the FIR selection

One basic difficulty of these studies based on individual galaxies is that the samples used are all biased and sometimes in a very complicated sense. The diagnostics on the UV slope of nearby galaxies all derive from the compilation of Kinney et al. (1993) of IUE observations of starburst galaxies which is not complete in any sense. Buat and Xu (1996) have used samples of star forming galaxies selected on their UV and FIR emissions leading to very complicated biases. Whereas the use of sample of galaxies which may be strongly biased is probably not a limitation to calibrate the physical link between the FIR to UV flux ratio and the extinction, the presence of these biases must be accounted for when generic properties of galaxies are deduced from these samples.

Our purpose is to use our FIR selected galaxy sample to test the influence of such a selection on the deduced value of the FIR to UV ratio. We will consider both fluxes at  $60 \mu\text{m}$  and in the range  $40\text{--}120 \mu\text{m}$ , the so-called FIR flux. Each one has its own advantages: on one hand more galaxies have a measured flux at  $60 \mu\text{m}$  than at  $100 \mu\text{m}$  and the luminosity function has been derived at  $60 \mu\text{m}$ , on the other hand the FIR emission over the range  $40\text{--}120 \mu\text{m}$  is more easily related to the total emission of the dust and hence to the amount of extinction than a single band flux.

In this section, we only discuss the observational biases and therefore use the data at  $60 \mu\text{m}$ . In figure 2 is reported

the ratio of fluxes at  $60 \mu\text{m}$  and  $0.2 \mu\text{m}$ ,  $F_{60}/F_{0.2}$  as a function of the flux and luminosity of the galaxies at  $60 \mu\text{m}$ .  $F_{60}$  and  $F_{0.2}$  are of the form  $F_\lambda = \lambda \cdot f_\lambda$  where  $f_\lambda$  is a flux per unit wavelength. The figure 2a with the flux of the galaxies can be used to study the selection bias in limited flux samples. The figure 2b where are reported the luminosities of the galaxies is useful to discuss the intrinsic properties of the galaxies.

There is a clear trend in both figures in the sense of a larger  $F_{60}/F_{0.2}$  ratio for brighter galaxies at  $60 \mu\text{m}$ . The tail found in figure 2a at large  $60 \mu\text{m}$  flux toward low  $F_{60}/F_{0.2}$  ratios is due to very nearby galaxies. This effect of distance disappears when the luminosity is considered (figure 2b). In order to highlight the general trend we have calculated a moving median on the sample. The data are sorted according to the  $60 \mu\text{m}$  luminosity, then a median is calculated for bins of 11 objects each time shifted by 5 objects. The result is shown in figure 3. As expected the moving median has reduced the dispersion of the data and flattened the dispersed trend of the figure 2b. A linear fit gives

$$\log(F_{60}/F_{0.2}) = 0.33(\pm 0.09) \log L_{60} - 2.60(\pm 0.19)$$

These figures illustrate the bias introduced by a FIR selection. As we consider galaxies with an increasing  $60 \mu\text{m}$  flux or luminosity, their  $F_{60}/F_{0.2}$  ratio also increases and is less and less representative of the mean properties of the local Universe as we will see below.

### 3.3. The galaxies detected at $60 \mu\text{m}$ and not at $0.2 \mu\text{m}$

The case of these galaxies is especially interesting since they are good candidates for very obscured galaxies. Nevertheless their low number (5 cases, section 2.2) makes them having no or little influence on the statistical properties discussed in this paper. Moreover, little information is known about these objects. Only one galaxy (F12242+0919) has a known redshift in the NED database.

The  $F_{60}/F_{0.2}$  ratio of each object is reported in table 2 and plotted in figure 2a. The upper limits found for these galaxies are compatible with the values found for some galaxies of the IRAS/FOCA sample but their location in the figure is surprising since they do not follow the general (although dispersed) trend of a larger  $F_{60}$  flux for a larger  $F_{60}/F_{0.2}$  ratio. However, only the figure 2b where the luminosity of the galaxies are reported has a physical meaning and unfortunately only one object (F12242+0919) has a measured redshift. Since F12235+0914 and F12259+1141 are classified by Yuan et al. as members of the Virgo cluster we assign them a distance of 17 Mpc. These three galaxies are reported in figure 2b. For the most luminous (F12242+0919) the upper limit of  $F_{60}/F_{0.2}$  is compatible with the general trend, the two faint Virgo dwarfs clearly disagree. Due to their faintness not much information is available for them, F12259+1141 is classified as dE and

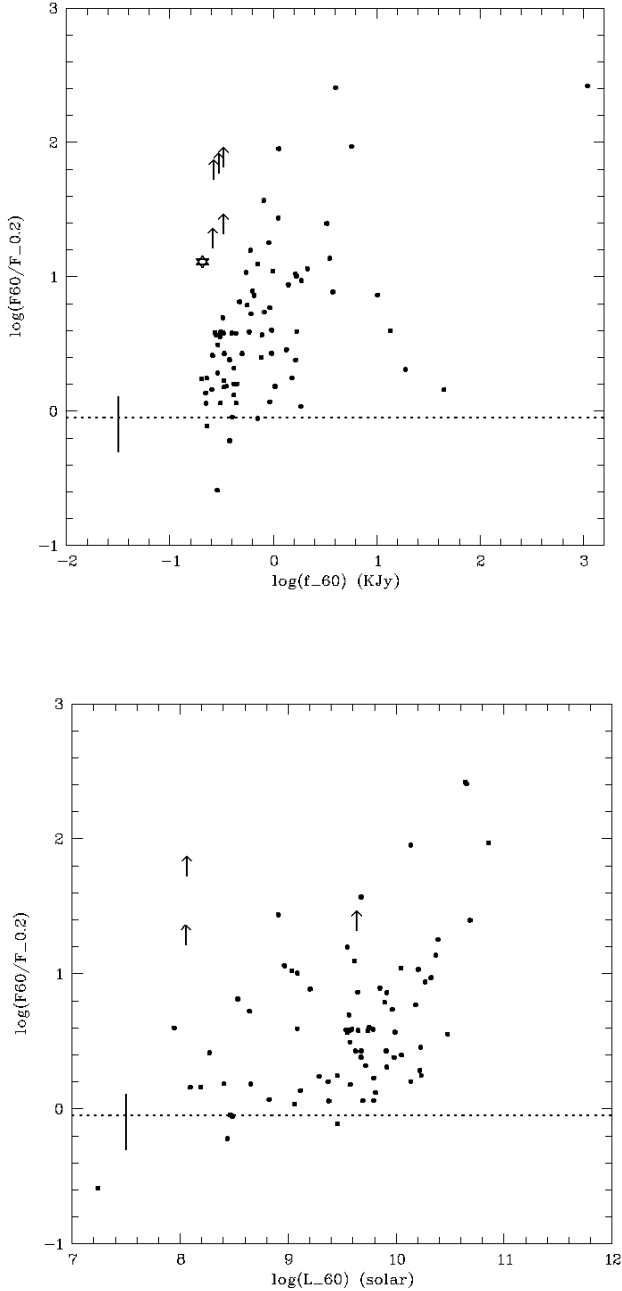


**Fig. 2.** The ratio of the emission at 60 and 0.2  $\mu\text{m}$  as a function of (a) the flux at 60  $\mu\text{m}$  and (b) the luminosity at 60  $\mu\text{m}$ . The ratio of the luminosity densities  $\rho_{60}/\rho_{0.2}$  is reported as a dotted horizontal line, the vertical line is the error bar

F12235+0914 dE or Im. A large FIR to UV ratio is not expected for elliptical galaxies, therefore these objects are probably not dE. We will see in section 6 that even the most FIR bright and extinguished objects known in the Uni-

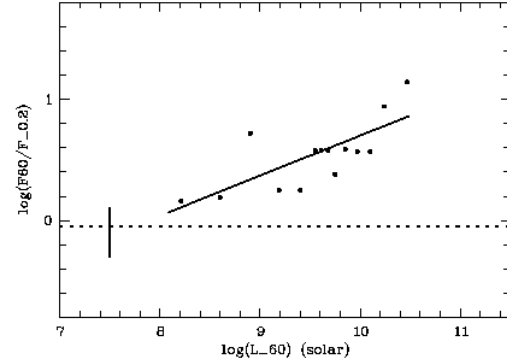


**Fig. 3.** The ratio of the emission at 60 and 0.2  $\mu\text{m}$  as a function of the luminosity at 60  $\mu\text{m}$  obtained with a moving median. The value reported on the X axis is the mean value of the 60  $\mu\text{m}$  luminosity within each bin. The linear fit is represented by the full line. The ratio of the luminosity densities  $\rho_{60}/\rho_{0.2}$  is reported as a dotted horizontal line, the vertical line is the error bar

verse follow and extend the trend found in figure 2b so the behavior of these two objects is difficult to understand.

We can try to estimate an extinction for the objects listed in table 2. Only two (F12041+6519, F13041+2907) have been detected at both 60 and 100  $\mu\text{m}$ . For these two galaxies we have the FIR flux to estimate the UV extinction (a lower limit for F13041+2907) using the formula (polynomial fit) established in section 3.1. For the galaxies not detected at 100  $\mu\text{m}$  we estimate arbitrarily this flux such as  $f_{60}/f_{100} = 0.3$  which is intermediate between the values for warm and cool dust (Lonsdale & Helou 1987), if this value is incompatible with the upper limit, we adopt the upper limit. The extinctions are listed in table 2. Adopting the relation of Meurer et al. leads to extinctions larger by 0.4 mag.

Three galaxies have a UV extinction larger than 3.5 mag, they are the two objects without any optical identification and the faintest galaxy of the table 2 detected in B. The three other cases (two non detections and the uncertain one) are less extreme ( $a_{UV} > \sim 2.5$  mag).

Note that the upper limits found for these galaxies are compatible with the values found for some galaxies of the IRAS/FOCA sample (figures 2). For example the two most extinguished galaxies of our sample, namely M82 and IC732, have a UV extinction larger than 5 mag and a  $F_{60}/F_{0.2}$  ratio larger than 2 in log unit.

#### 4. Comparison with the luminosity functions and densities in the local universe

#### 4.1. The ratio of the luminosity densities

The luminosity functions and luminosity densities of the local universe are available at both wavelengths (0.2 and 60  $\mu\text{m}$ ). Therefore we can compare some of their properties to the characteristics of individual galaxies. The 60  $\mu\text{m}$  local luminosity function and density at  $z=0$  have been calculated by Saunders et al. (1990). The 0.2  $\mu\text{m}$  luminosity function and density have been derived by Treyer et al. (1998) at a mean  $z=0.15$ . From these studies we can calculate the ratio of the local luminosity densities  $\rho_{60}/\rho_{0.2}$  at  $z=0$ . To this aim we correct the UV density for the redshift evolution. From Madau et al. (1998) we estimate that the luminosity density increases by a factor  $\sim 1.5 \pm 0.2$  from  $z=0$  to  $z=0.15$  which is consistent with the estimates of Lilly et al. (1996) and Cowie et al. (1999). Applying this factor to the estimate of Treyer et al. we obtain  $\rho_{0.2} = 4.6 \pm 2.0 \cdot 10^7 \text{ h L } \odot / \text{Mpc}^3$ . With  $\rho_{60} = 4.2 \pm 0.4 \cdot 10^7 \text{ h L } \odot / \text{Mpc}^3$  we find  $\rho_{60}/\rho_{0.2} = 0.9 \pm 0.4$  at  $z=0$ . In the same way, from  $\rho_{\text{FIR}} = 5.6 \pm 0.6 \cdot 10^7 \text{ h L } \odot / \text{Mpc}^3$  (Saunders et al. 1990), we calculate  $\rho_{\text{FIR}}/\rho_{0.2} = 1.2 \pm 0.5$ .

$\rho_{60}/\rho_{0.2}$  is reported in figures 2 and 3. The ratio appears lower than almost all the ratios found for individual galaxies and is systematically lower than all the median values calculated for increasing 60  $\mu\text{m}$  luminosity (figure 3). *Therefore the study of individual galaxies of our sample does not lead to a reliable estimate of the mean FIR to UV ratio of the local Universe.*

Our sample is FIR selected since we have searched for FIR galaxies detected in UV, therefore a bias toward large FIR to UV flux ratio is expected and this bias increases as we select brighter galaxies (figure 2). For comparison, we can also re-consider the sample used by Buat & Xu (1996) : the galaxies were primarily selected to have a UV measurement and then searched in the IRAS database. Only galaxies detected both in UV and FIR are considered. Whereas the selection biases of this sample are very complicated since the primary selection is on the UV the bias toward the FIR is certainly less strong than for the IRAS/FOCA sample.

In figure 4 the histograms of  $F_{\text{FIR}}/F_{\text{UV}}$  ratio are reported for three samples: the IRAS/FOCA sample (solid line), the IUE/IRAS templates of Meurer et al. (1999) (dotted line) and the sample of Buat & Xu (dashed line). We can see that almost all the IRAS/FOCA galaxies and the local IUE/IRAS templates exhibit a larger ratio than the ratio of the local luminosity densities  $\rho_{\text{FIR}}/\rho_{0.2}$ . The situation is less extreme for the Buat & Xu sample for which the median of the  $F_{\text{FIR}}/F_{\text{UV}}$  flux ratio is 1.66, translating to  $a_{0.2} = 0.71 \text{ mag}$  (0.94 mag with the formula of Meurer et al.). This difference in the FIR and UV properties of the samples explains the rather low extinction found by Buat & Xu for this sample as compared with those obtained by Meurer et al.

The mean property of the local Universe in terms FIR to UV luminosity density ratio is not well represented by

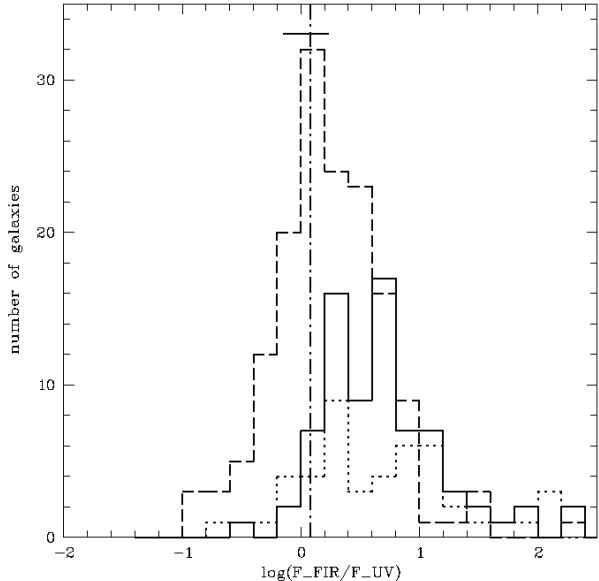


**Fig. 4.** The ratio of the FIR and UV fluxes for different samples of galaxies: the IRAS/FOCA sample (solid line) and the sample of Buat & Xu (1996) (dashed line) with UV fluxes taken at 0.2  $\mu\text{m}$ , the IUE/IRAS templates of Meurer et al. (1999) (dotted line) with UV fluxes taken at 0.16  $\mu\text{m}$ . The vertical dot-dashed line is the location of  $\rho_{\text{FIR}}/\rho_{0.2}$ , the horizontal line is the error bar

the samples of galaxies considered here. Therefore much caution must be taken to estimate global correction for extinction to be applied to the luminosity function.

#### 4.2. The local luminosity functions

An explanation for the discrepancy between the  $F_{60}/F_{0.2}$  ratio of individual galaxies and the ratio of the local luminosity densities is that it is not the same galaxies which form the bulk of the UV emission on one hand and the FIR emission on the other hand. Indeed, the large difference found in the shape of the two luminosity functions is consistent with this explanation as already discussed in Buat & Burgarella (1998). The adopted value of  $\rho_{60}/\rho_{0.2}$  depends on the reliability of the luminosity functions and is subject to some uncertainties. Nevertheless very large modifications must be invoked to make consistent the  $F_{60}/F_{0.2}$  ratios in our IRAS/FOCA sample and the mean value of the local universe. Moreover it would not explain the trend found of an increase of the  $F_{60}/F_{0.2}$  ratio with the FIR luminosity of the galaxies.

We have evaluated the contribution to the luminosity function and the luminosity density at 0.2  $\mu\text{m}$  (resp. 60  $\mu\text{m}$ ) of the galaxies as a function of their intrinsic luminosity (per decade of luminosity). These values are re-

ported in table 3 (resp 4) together with the number of galaxies of our IRAS/FOCA sample in each bin of luminosity (in log unit). The luminosity functions are truncated at  $L = 10^7 L_{\odot}$ .

As expected for a magnitude limited sample, our individual galaxies do not truly sample the luminosity functions. This effect is dramatic in UV: the steepness of the faint end slope of the UV luminosity function (Treyer et al. 1998) implies a large number of faint galaxies. These objects largely contribute to the UV luminosity density. The relative numbers of galaxies in each bin of UV luminosity are similar to those used by Treyer et al. to calculate the UV luminosity function.

Conversely, the FIR luminosity function is better sampled in the sense that the deficiency of low luminosity galaxies has less implications than in UV. Indeed, the FIR luminosity function is extremely flat at low luminosities (Saunders et al. 1990) and the contribution of the faint FIR galaxies to the local luminosity density is very low. As a consequence the number of galaxies in each bin of luminosity is more representative of its contribution to the FIR luminosity density than in UV. The bright end of both luminosity functions is not represented in the IRAS/FOCA sample because of the scarcity of these objects and the small statistics. In terms of global (cumulated) luminosity of our sample of individual galaxies we are entirely dominated by the galaxies between  $10^9$  and  $10^{11} L_{\odot}$  at both wavelengths (0.2 and  $60 \mu\text{m}$ ) but this does not influence our results since each galaxy is considered individually whatever its luminosity is, without any summation on individual objects.

Hence our sample IRAS/FOCA sample of individual galaxies is more representative of the FIR properties of the universe. If the faint UV galaxies are dwarf galaxies they probably have a low extinction and therefore a low FIR to UV ratio. Our sample being FIR selected, it is probably biased against these objects.

A consequence of these effects is that when a correction for extinction is calculated from individual galaxies using such a correction to correct the entire luminosity function can lead to some mistakes as we will discuss in the next subsection.

#### 4.3. Consequences on the estimate of the UV extinction for large samples of galaxies and statistical studies

Most of the time neither the FIR flux nor the UV continuum ( $\beta$  slope) are available for large and/or deep surveys of galaxies and one cannot use these dust extinction calibrators. The situation is better at high  $z$  due to the redshifting of the UV continuum. For instance Meurer et al. (1999) have performed individual corrections on the Lyman break U-dropouts galaxies at  $z \simeq 3$  in the HDF by estimating the  $\beta$  slope from the V and I measurements. Nevertheless they sampled only bright galaxies ( $M_{AB} < \sim -19$

i.e. whose UV luminosity is larger than  $810^9 L_{\odot}$ ) since only such bright objects are reachable at high  $z$ .

The problem of the correction for extinction arises when one has to derive an intrinsic UV luminosity distribution (Treyer et al. 1998, Steidel et al. 1999). At low redshift the UV slope is not available for the moment on a large sample of galaxies and cannot be used to correct the UV luminosity function for dust extinction. The extinction has been found to vary as a function of the absolute bolometric magnitude of the galaxies (e.g. Wang 1991, Heckman et al. 1998, Buat & Burgarella 1998). Unfortunately, the UV luminosity is not a good tracer of the bolometric luminosity of a galaxy since it is expected to be very influenced by the current star formation activity. Moreover the extinction (larger for brighter galaxies) adds an anti correlation between the observed UV luminosity and the bolometric one. Therefore, relating the extinction to the UV luminosity is not possible. Indeed no correlation exists between the UV luminosity and the FIR/UV ratio in the IRAS/FOCA sample or that previously used by Buat & Xu (1996). In the same way Heckman et al. (1998) have used the sum of the FIR and UV luminosities as a tracer of the bolometric luminosity.

The use of the absolute B magnitude  $M_B$  is also far from ideal since it suffers from the same caveats as the UV luminosity (star formation history and extinction), although in a less extreme way. Actually a trend has been found between the ratio of the dust to UV emission and  $M_B$  for a sample of nearby starburst galaxies (Buat & Burgarella 1998) but the relation is too dispersed to be used as a quantitative calibrator of the extinction. More promising is the use of data at longer wavelengths like the R or I band: the effects of extinction will be largely reduced and we can hope to better trace the mass of the galaxies. Such investigations are devoted to a subsequent paper.

We have also compared the extinction deduced from the FIR/UV flux ratio ( $a_{0.2}$ , section 3.1) to the UV-B color since this color is often available for large samples (e.g. Treyer et al. 1998). The extinction is plotted against the UV-B color for our IRAS/FOCA sample in figure 5.

A correlation is found between these two quantities ( $R=0.70$ ). Indeed, a clear correlation has already been found between the FIR/UV flux ratio and the UV-B color (Deharveng et al. 1994) which has been interpreted to be due at least in part to the influence of the dust extinction (Buat et al. 1997). The UV-B color is also sensitive to the star formation history on timescales of the order of some  $10^9$  years: it is likely to be at the origin of the dispersion found in figure 5 and only rough tendencies can be securely deduced. Nevertheless, it appears necessary to account for the variation of the extinction among galaxies which can vary by three magnitudes. In particular galaxies with a UV-B color lower than  $\sim -2$  are very little affected by the extinction and it would seem reasonable to apply no correction of extinction to them.



**Table 3.** Contribution of the galaxies to the UV luminosity function and to the UV luminosity density in the local Universe per decade of luminosity. The luminosity function is truncated at  $L = 10^7 L_{\odot}$  ( $h = 0.75$ ).

$\log(L_{UV})$ solar unit	percentage of galaxies from the luminosity function	relative contribution to the local UV density	percentage of galaxies in the IRAS/FOCA sample
7-8	77.3%	17 %	11%
8-9	19.3%	36%	33%
9-10	3.2 %	36%	56%
10-11	0.2 %	11%	0%

**Table 4.** Same as table 3 at  $60 \mu\text{m}$

$\log(L_{60})$ solar unit	percentage of galaxies from the luminosity function	relative contribution to the local $60\mu\text{m}$ density	percentage of galaxies in the IRAS/FOCA sample
7-8	45.4 %	2%	3%
8-9	35.6 %	15%	17%
9-10	16.2 %	40%	56%
10-11	2.7 %	34%	24%
11-12	0.1 %	8%	0%

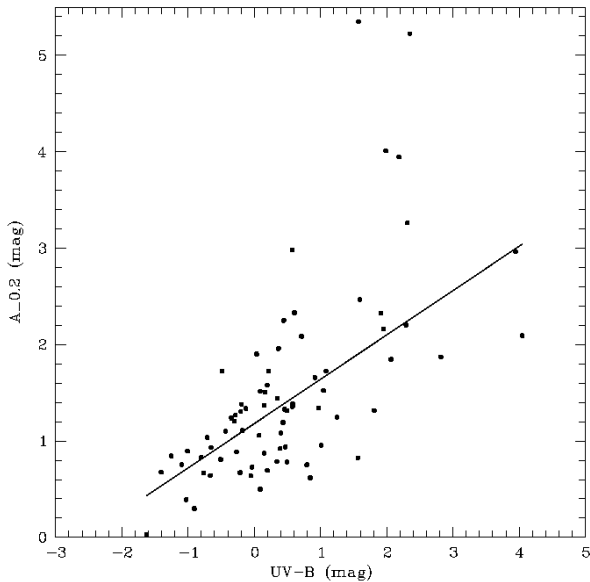


**Fig. 5.** The UV extinction at  $0.2 \mu\text{m}$  calculated with the FIR to UV flux ratio of galaxies as a function of the UV-B color for the IRAS/FOCA sample. The solid line is the result of a linear regression:  $a_{0.2} = 1.18(\pm 0.58) + 0.46(\pm 0.06)(UV - B)$

## 5. Estimating star formation rates

Both FIR and UV emissions are powerful star formation tracers. To derive reliable star formation rates (SFRs) one must account for the repartition of the emission of young stars in both wavelength ranges since the stellar emission lost by dust extinction is re-emitted in the FIR.

As already proposed by Heckman et al. (1998), perhaps the best way is to consider both UV and FIR emissions: each emission can be related to the star formation rate and the sum of the two SFRs deduced from the FIR and the UV should account for the total emission of young stars.

In such an approach the uncertainty resides in the translation of the UV and FIR emissions into quantitative star formation rate. The UV flux is directly proportional to the star formation rate provided that the star formation has been constant for some  $10^8$  years and assuming a universal initial mass function (IMF). We have used the models of Leitherer et al. (1999) for different IMFs (Salpeter IMF (-2.35) or -2.5, upper mass limit 100 or  $125 M_{\odot}$  for a lower mass limit equal to  $0.1 M_{\odot}$ ). The metallicity is taken solar. After  $5 \cdot 10^8$  years of constant star formation the production of the UV luminosity reaches stationarity:  $\text{SFR}(M_{\odot}/\text{yr}) = 2.7 \cdot 10^{-10} L_{UV}(L_{\odot})$  at  $0.2 \mu\text{m}$  for a Salpeter IMF and an upper mass limit of  $125 M_{\odot}$ . Nevertheless after  $5 \cdot 10^7$  years the UV luminosity reaches more than 80% of this stationary value. For the same IMF, using Madau estimations (1998) based on the models of Bruzual & Charlot Treyer et al. (1998) have adopted a conversion factor  $\text{SFR}/L_{UV}$  equal to  $3.36 \cdot 10^{-10} M_{\odot} \text{ yr}^{-1} / L_{\odot}$  i.e. a difference of 20%. The uncertainty due to the IMF is around  $\sim 40\%$ . Therefore we can conservatively estimate that the uncertainty on the conversion of the UV luminosity in star formation rate is 50% provided that the galaxy has formed stars continuously for some  $10^7$  years.

The link between the SFR and the FIR luminosity is more indirect than for the UV luminosity since it depends of the dust heating which involves all types of stars. Nevertheless, in starbursting galaxies the situation is expected to be less complex since the dust heating is

dominated by the young stars. Under such conditions Kennicutt (1998) has related the FIR luminosity to the star formation rate  $\text{SFR} = 1.71 \cdot 10^{-10} L_{\text{FIR}}(L_{\odot})$  where  $L_{\text{FIR}}$  is the total FIR luminosity. This conversion factor  $\text{SFR}/L_{\text{FIR}}$  is obtained using synthesis population models and is also subject to uncertainties on the stellar tracks, the IMF or the star formation history. From a comparison with the calculations of Lehnert & Heckman (1996), Meurer et al. (1997) and Buat & Xu (1996) we estimate the uncertainty of the order of 50% for  $\text{SFR}/L_{\text{FIR}}$ .

Therefore we can reasonably estimate that the SFR deduced from the observed UV luminosity added to that deduced from the FIR one is also uncertain by a factor  $\sim 50\%$ . Nevertheless it must be noticed that the conversion formulae only apply to galaxies which have experimented a continuous star formation for at least  $\sim 10^8$  years and will not be valid for galaxies with more episodic star formation, especially post starbursting galaxies.

### 5.1. The IRAS/FOCA sample

The IRAS/FOCA sample is FIR selected, thus it is biased against very blue dwarf galaxies which may exhibit episodic bursts of star formation as suggested by Fioc & Rocca-Volmerange (1999). Therefore we can expect that the derivation of a SFR from the FIR and UV emissions is valid for this sample of galaxies. The comparison of the star formation rates obtained by adding the FIR and UV (observed) emissions to those deduced from the UV fluxes after a correction for extinction can be useful to test the consistency of both methods. Therefore we have calculated the star formation rates for the IRAS/FOCA sample of galaxies adding the contribution of the FIR and UV (not corrected for extinction) emissions and using the conversion formula of Treyer et al. (1998) for the UV and Kennicutt (1998) for the FIR. Total FIR fluxes have been estimated using the relation found by Buat & Burgarella (1998) between the ratio of the total dust flux to the FIR (40-120 $\mu\text{m}$ ) flux and  $f_{60}/f_{100}$ . The estimated SFRs can be compared to the ones obtained after correction of the UV fluxes from extinction. The correlation between the two estimates is very good but the SFRs deduced from the (FIR + UV) emissions are higher than the SFRs deduced from the UV corrected emission by a factor 1.4. Another interesting comparison is that of the relative contribution of the UV (not corrected for extinction) and FIR emissions to the total (FIR + UV) SFR. For our sample of IRAS/FOCA galaxies the relative contribution of the UV and FIR emissions to the total SFR are 0.3 and 0.7 respectively. However, these calculations assume that the FIR flux is exclusively due to the heating by young stars. Since all our galaxies are certainly not starbursting objects the contribution of the emission of dust heated by old evolved stars must be deduced from the FIR flux before translating it into star formation rate reducing the contribution of

the FIR emission to the SFR. Let us assume that old stars contribute for 30 % of the dust heating (Xu 1990, Buat & Xu 1996), then the ratio of the SFR deduced from the (FIR + UV) emissions and the SFR deduced from the UV corrected emission is reduced from 1.4 to 1.1 and the relative contributions of the UV and FIR emissions to the total SFR are now 0.4 and 0.6.

Given all the uncertainties inherent to these calculations we must be cautious in our conclusions. We can say that the corrections for dust extinction deduced from the FIR/UV flux ratio and applied to the UV observed emissions lead to a SFR consistent with that obtained by adding the SFRs deduced from both the FIR and observed UV emissions. This makes us confident in our estimate of the extinction.

### 5.2. The local volume-average star formation rate

Under the hypothesis of an average star formation of the local universe continuous over  $\sim 10^8$  years, we can derive global star formation rates from the local FIR and UV luminosity densities:

$$\rho_{\text{SFR}} = \rho_{\text{SFR}}^{\text{FIR}} + \rho_{\text{SFR}}^{\text{UV}}$$

$\rho_{\text{SFR}}^{\text{FIR}}$  is calculated using the value of  $\rho_{\text{FIR}}$  (section 4.1) multiplied by 1.5 to account for the total dust luminosity density (e.g. Xu & Buat 1995, Meurer et al. 1999);  $\rho_{\text{SFR}}^{\text{UV}}$  is calculated from  $\rho_{0.2}$ . We find:

$$\rho_{\text{SFR}} = (0.014 + 0.015)(\pm 0.01) \text{ h} \cdot \text{M}_{\odot} / \text{yr} / \text{Mpc}^3$$

This time the contributions of the FIR and UV are very similar, this is due to the lower value of the FIR to UV density ratio as compared to the FIR to UV flux ratio of individual galaxies. Then the volume-average star formation rate deduced from the UV luminosity density not corrected for dust extinction must be multiplied by a factor  $\sim 2$  to account for the global extinction, this corresponds to a mean extinction of 0.75 mag at 0.2  $\mu\text{m}$ . As discussed before this rather low value is due to the contribution of faint blue galaxies to the UV luminosity density. Actually, using the  $\rho_{\text{FIR}}/\rho_{0.2}$  ratio gives an extinction of 0.77 mag using the model of Meurer et al. and 0.55 mag for our polynomial fit (section 3.1) As already underlined, the difference is likely to come from the contribution of the old stars to the dust heating: let us assume that 30% of the FIR emission comes from these old stars and is not related to the recent star formation then we find that  $\sim 40\%$  of the star formation is locked in FIR and 60% in UV. The resulting UV extinction is 0.58 mag and  $\rho_{\text{SFR}} = 0.025 \text{ h} \text{ M}_{\odot} / \text{yr} / \text{Mpc}^3$ .

Therefore we can conclude that the derivation of the global star formation rate is in agreement with our estimate of the global extinction in UV and that the same amount of star formation rate is traced by the global FIR

and UV (not corrected for extinction) luminosity densities.

## 6. Comparison with FIR bright galaxies

Since the IRAS survey, FIR bright galaxies have been the subject of numerous studies because these objects experiment an intense star formation activity. The extreme case is that of UltraLuminous Infrared Galaxies (ULIGs) with a bolometric luminosity larger than  $10^{12} M_{\odot} / \text{yr}$  essentially emitted in FIR and star formation rates of several hundreds solar masses per year: they generally are violent mergers and may represent an important phase in the formation of large galaxies like ellipticals (Mirabel & Sanders 1996). Such objects are known to be rare at low  $z$  but they might be far more numerous at high  $z$  as suggested by the sub millimetric surveys with SCUBA (e.g. Sanders 1999).

With the launch of the ISO satellite, the sensitivity of the ISOCAM camera has allowed mid-infrared surveys at intermediate redshift ( $z < 1$ ). In particular Flores et al. (1998) have observed one CFRS field, therefore UV ( $0.28 \mu\text{m}$ ) and infrared data are available for these galaxies.

We now compare the FIR and UV properties of these galaxies (ULIG and ISOCAM/CFRS) to that of our IRAS/FOCA sample of nearby galaxies. The comparison is rather straightforward since all these objects are IR selected.

### 6.1. Ultraluminous Infrared Galaxies (ULIG)

#### 6.1.1. nearby ULIGs

Trentham et al. (1999) have obtained HST observations for three ultra luminous infrared galaxies: VII Zw031, IRAS F12112+0305, IRAS F22491-1808. These galaxies are selected to be cool in order to avoid a non thermal origin for the FIR emission. We can calculate directly their  $L_{60}/L_{UV}$  ratio using the data at  $0.23 \mu\text{m}$  for the UV emission. The three objects are reported in figure 6 (similar to fig.2b) with empty stars for symbols. As expected for this type of objects they appear to be very luminous at  $60 \mu\text{m}$  with a high FIR to UV flux ratio. Such objects are not represented in our FIR selected sample of nearby galaxies: this emphasizes how much these objects are rare in the local Universe and with extreme properties as often underlined (e.g. Sanders & Mirabel 1999). Since the three ULIG have also been detected at  $100 \mu\text{m}$  we can estimate their UV extinction (we neglect the difference in the UV wavelengths i.e.  $0.23 \mu\text{m}$  versus  $0.2 \mu\text{m}$ ). We find  $\sim 6.5$  mag: more than 99% of the UV flux of these objects is emitted in the FIR.

#### 6.1.2. High redshift galaxies detected by SCUBA : ULIG candidates

Hughes et al. (1998) have observed the HDF field at  $850 \mu\text{m}$  with SCUBA. 5 objects detected by SCUBA

in the HDF field have been tentatively associated to optical sources for which photometric redshift are available but such an identification is difficult because of the uncertainty on the  $850 \mu\text{m}$  positions. Indeed, the identification of the most brightest source (HDF850.1) has not been confirmed (Sanders, 1999). Moreover the nature of these sources, starbursts or AGN, is not clear: at FIR luminosity larger than  $10^{12} L_{\odot}$  about half of the nearby ULIGs are predominantly powered by AGNs (e.g. Sanders 1999).

The  $60 \mu\text{m}$  luminosity of the 4 remaining galaxies is obtained from their emission at  $850 \mu\text{m}$  accounting for the redshifting and an assumed spectral energy distribution chosen to be that of M82. The optical data from the HDF lead to the estimate of the UV flux at a rest frame wavelength of  $0.28 \mu\text{m}$ . All these estimates rely on the resemblance of all ULIGs with M82 and can lead to false results (e.g. Sanders 1999). In spite of these caveats, we have reported the 4 high redshift galaxies in figure 6 (filled triangles). They appear very extreme, being more luminous in FIR and probably more extinguished than all the other galaxies studied in this paper. A tentative estimate of the extinction is obtained by using the  $F_{60}/F_{UV}$  instead of the  $F_{FIR}/F_{UV}$  one. We find values spanning from 8 to 11 mag. As a comparison M82, which belongs to our IRAS/FOCA sample exhibit "only" 5.4 mag of extinction at  $0.2 \mu\text{m}$ . These high redshift ULIGs seem also to be much more extinguished than the most luminous Lyman break galaxies of the HDF studied by Meurer et al. (1999) for which they derive an extinction not larger than 3.5 mag. Although their UV luminosity corrected for extinction are comparable ( $\sim 10^{12} L_{\odot}$ ), these two classes of galaxies do not seem to exhibit the same properties in FIR and UV as suggested by Heckman (1999). Indeed we can try to roughly locate the most luminous galaxies of Meurer et al. in figure 6. The FIR luminosity can be estimated from their star formation rates and the  $F_{60}/F_{UV}$  ratio from their extinction using the figure 1. It gives  $L_{60} \sim 10^{12} L_{\odot}$  and  $F_{60}/F_{UV} \sim 1.2 - 1.4$  for an extinction of  $\sim 3$  mag. Therefore it seems that the Lyman Break Galaxies detected in the HDF by their U-dropout do not follow the steep trend of figure 6 found for FIR bright galaxies but instead exhibit a lower increase of the extinction with the intrinsic luminosity of the galaxies. Such a difference may be due to the contribution of AGNs in ULIGs. Indeed the extrapolation of the mean trend found in the IRAS/FOCA sample (figure 3) reported as a full line in the figure 6 does not lead to the extreme case of ULIGs and seems more compatible with LBGs.

### 6.2. ISOCAM/CFRS galaxies

Flores et al. (1998) have obtained ISO/ISOCAM Mid Infrared images of one CFRS field, most of the detections are at  $15 \mu\text{m}$ . The infrared  $8-1000 \mu\text{m}$  luminosities have

been deduced from MIR and/or radio measurements using templates of spectral energy distributions and are probably not very secure but an approximate value is sufficient for our comparison with local templates. We differentiate AGNs and starbursts as classified by Flores et al. Only the global IR (8-1000  $\mu\text{m}$ ) flux is available for these objects and not the flux at 60  $\mu\text{m}$ . We adopt a mean value of  $\sim 1.5$  for the ratio of the total dust emission to that intercepted by the 40-120  $\mu\text{m}$  band (see section 5.2). Then we estimate the ratio between the flux at 60  $\mu\text{m}$  and the FIR (40-120  $\mu\text{m}$ ) for our IRAS/FOCA sample:  $L_{60}/L_{\text{FIR}} = 0.84 \pm 0.12$ . Therefore the total IR fluxes given by Flores et al. have been divided by a factor 2 in order to roughly represent the flux at 60  $\mu\text{m}$ .

The UV emission is taken at 0.28  $\mu\text{m}$  as given by Flores et al. It is difficult to estimate a correction factor to translate the UV data to 0.2  $\mu\text{m}$  in the absence of observations of a large sample of galaxies at both wavelengths since the ratio depends on the star formation history and the dust extinction. We can try to use synthesis models for this estimate: assuming a constant star formation rate over 1 Gyr and using the models of Leitherer et al. (1999) for a solar metallicity we find  $F_{0.2}/F_{0.28} = 1.7$  the flux being defined as  $\lambda \cdot f_{\lambda}$ . The difference of extinction between 0.28 and 0.2  $\mu\text{m}$  has been calculated using the extinction curves of the Milky Way and the LMC (Pei 1992) and that of Calzetti (1997). The ratio  $A_{0.2}/A_{0.28} = 1.2 - 1.4$ . Therefore the two effects (star formation and extinction) roughly compensate each other and we do not perform any correction between 0.28 and 0.2  $\mu\text{m}$ . The galaxies are plotted in figure 6 as crosses for the true starbursts and empty circles for the Seyferts. They all fill the gap between the IRAS/FOCA sample and the ULIGs. Therefore, they are not as extreme as ULIGs but their extinction is larger than the nearby galaxies of the IRAS/FOCA sample. For the galaxies classified as starbursts, we have tentatively estimated this extinction from their FIR to UV flux ratio. The extinctions found span from 2 to 5.5 with a mean at 3.3 mag (and a median at 3 mag). This is much larger than that estimated by Flores et al. by matching the global star formation rates deduced from the total FIR and the UV luminosities in the observed field: they find extinctions around 2 mag at 0.28  $\mu\text{m}$ . This discrepancy between the extinction occurring in individual galaxies selected in infrared and that deduced from the total FIR and UV luminosity of a selected field (i.e. the sum of the luminosity of all galaxies detected in the wavelength band (FIR or UV)) is well illustrated in the table 5 of Flores et al. where the ratio  $L_{\text{IR}}/L(0.28\mu\text{m})$  calculated for individual objects observed at both 15 and 0.28  $\mu\text{m}$  is  $\sim 5$  times larger than the ratio of the global luminosities IR and UV luminosities in the CFRS field. This is in full agreement with our own results presented in section 4.

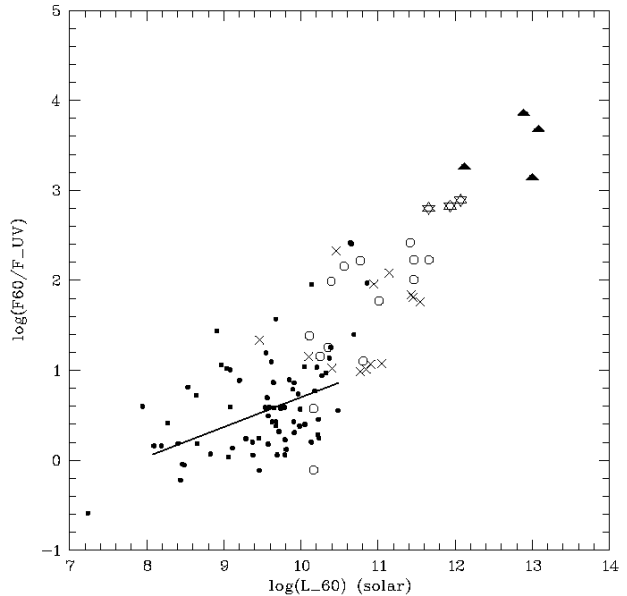


**Fig. 6.** FIR bright galaxies are superposed to our IRAS/FOCA sample (dots): ISOCAM/CFRS starburst galaxies with crosses, ISOCAM/CFRS active galaxies with empty circles, nearby ULIGs with stars and distant SCUBA detections with filled triangles ( $h=0.75$ ).

## 7. Conclusions

We have constructed a sample of 102 nearby galaxies detected by IRAS at 60  $\mu\text{m}$  and for which UV observations at 0.2  $\mu\text{m}$  are available down to  $m_{\text{UV}} \sim 17 - 18$ . Only five galaxies have no UV detection implying an extinction larger than 2-3 mag for these objects which are also very faint in FIR.

The FIR and UV properties of our sample have been compared to the mean properties of the local Universe deduced from the luminosity functions and densities at both wavelengths. As the galaxies become brighter in FIR their FIR to UV flux ratio, i.e. their extinction increases:  $d(\log(L_{60}/L_{0.2}))/d(\log L_{60}) \simeq 0.3$  which translates to an increase of  $\sim 0.5$  mag for the dust extinction in UV per decade of FIR luminosity.

The ratio of the FIR to UV local luminosity densities is much lower than that found in individual galaxies. It is also true for other samples of nearby galaxies usually considered as low redshift templates like the IUE sample of Calzetti Kinney and collaborators. Such a difference is likely to be due to the large contribution of low UV luminosity galaxies to the UV luminosity density: these galaxies are deficient in any survey. At FIR wavelengths such faint galaxies do not significantly contribute and our sample is more representative of the galaxy population in terms of its contribution to the FIR luminosity density. As a consequence, much caution must be taken to correct

large samples of galaxies for extinction. In particular a uniform correction deduced from the study of some individual cases cannot be valid.

Star formation rates can be estimated by accounting for both the FIR and UV emissions: each one is translated to a quantitative SFR; then, the two SFRs are summed. The SFRs such deduced are consistent with those calculated from the UV emission corrected for extinction.

A local volume-average star formation rate is calculated from the FIR and UV luminosity density:  $\rho_{\text{SFR}} = 0.03 \pm 0.01 \text{ h} \cdot \text{M} \odot / \text{yr} / \text{Mpc}^3$ . This is consistent with a global extinction of  $\sim 0.6$  mag at  $0.2 \mu\text{m}$ .

Endly, we have compared the FIR and UV properties of our sample of galaxies to those of nearby and high redshift UltraLuminous Infrared Galaxies observed both at UV and FIR rest frame wavelengths and to the ISOCAM survey of a CFRS field. All these objects extend toward the large luminosities the trend found for the nearby galaxies of a larger FIR to UV ratio for brighter galaxies. The ULIGs are very extreme with UV extinctions reaching 8-11 mag. Although more moderate the extinctions we find for the ISOCAM/CFRS objects not classified as Seyfert are comprised between 2 and 5.5 mag. These calculations are only tentative due to the large uncertainties about the FIR emission of these objects.

*Acknowledgements.* We thank J.-M. Deharveng and M. Treyer for their careful reading of the manuscript and A. Boselli for helpful and stimulating discussions about this work as well as for his help in the study of individual objects.

## References

- Buat V., Burgarella D., 1998, A&A 334, 772  
 Buat V., Burgarella D., Xu C., 1997, The Ultraviolet Universe at low and high redshift, eds. M. Fanelli & B. Waller, AIP conference proceedings 408, 379  
 Buat V., Xu C., 1996, A&A 306, 61  
 Calzetti D., 1997, The Ultraviolet Universe at low and high redshift, eds. M. Fanelli & B. Waller, AIP conference proceedings 408, 403  
 Calzetti D., Kinney A.L., Storchi-Bergman T., 1994, ApJ 429, 582  
 Cowie L.L., Songaila A., Barger A.J., 1999, astro-ph/9904345  
 Deharveng J.M., Sasseen T.P., Buat V., Bowyer S., Wu X., 1994, A&A 289, 71  
 Donas J., Milliard B., Laget M., 1991, A&A 252, 487  
 Fioc M., Rocca-Volmerange B., 1999, A&A 344, 393  
 Flores H., Hammer F., Thuan T., Césarsky C., Désert F.X., Omont A., Lilly S.J., Eales S., Crampton D., Le Fèvre O., 1998, ApJ 517, 148  
 Heckman T., 1999, astro-ph/9903041  
 Heckman T., Robert C., Leitherer C., Garnett D., van der Rydt F., 1998, ApJ 503, 646  
 Helou G., Khan I.R., Malek L., Boehmer L., 1988, ApJS, 68, 151  
 Hughes D.H., Serjeant S., Dunlop J. et al., 1998, Nature 394, 241  
 Kennicutt R.C., 1998, ApJ 498, 541  
 Kinney A.L., Bohlin R.C., Calzetti D., Panagia N., Wyse R., 1993, ApJS 86, 5  
 Kinney A.L., Calzetti D., Bica E., Storchi-Bergman T., 1994, ApJ 429, 17  
 Lehnert M.D., Heckman T.M., 1996, ApJ 472, 546  
 Leitherer C., Schaerer D., Goldader J.D. et al., 1999, ApJS in press  
 Lilly S., Le Fèvre O., Hammer F., Crampton D., 1996, ApJ 460, L1  
 Lonsdale C.J., Helou G., 1987, ApJ 314, 513  
 Madau P., Pozzetti L., Dickinson M., 1998, ApJ 498, 106  
 Meurer G.R., Heckman T.M., Calzetti D., 1999, ApJ 521, 64  
 Meurer G.R., Heckman T.M., Lehnert M.D., Leitherer C., Lowenthal J., 1997 AJ 114, 54  
 Meurer G.R., Heckman T.M., Leitherer C., Kinney A., Robert C., Garnett D.R., 1995, AJ 110, 2665  
 Milliard B., Donas J., Laget M., Huguenin D., 1994, *The balloon-borne 40-cm UV-(200 nm) imaging telescope FOCA: results and perspective*, 11th ESA Symposium, Montreux, ESA SP.  
 Pei Y.C., 1992, ApJ 395, 130  
 Pettini M., Kellogg M., Steidel C.C., Dickinson M., Adelberger K.L., Giavalisco M., 1998, ApJ 508, 539  
 Sanders D.B., 1999, astro-ph/9904292  
 Sanders D.B., Mirabel I.F., 1996, ARAA 34, 749  
 Saunders W., Rowan-Robinson M., Lawrence A. et al., 1990, MNRAS 242, 318  
 Steidel, C.C., Adelberger, K.L., Giavalisco, M., Dickinson, M., Pettini, M., 1999, ApJ 519, 1  
 Trentham N., Kormendy J., Sanders D., 1999, AJ 117, 2152  
 Treyer M.A., Ellis R.S., Milliard B., Donas J., Bridges T.J., 1998, MNRAS 300, 303  
 Wang B., 1991, ApJ 383, L37  
 Witt A. N., Gordon K. D. 1999 astro-ph/9907342  
 Xu C., 1990, ApJ 365, L47  
 Xu C., Buat V., 1995, A&A 293, L65  
 Yuan Q.R., Zhu Z.H., Yang Z.L., Hu X.T., 1996, A&AS 128, 299